FUSE

Fungal Systematics and Evolution

VOLUME 15
JUNE 2025
PAGES 79–96

doi.org/10.3114/fuse.2025.15.03

Novel amplified fragment length polymorphism (AFLP) markers for typing medically relevant *Fusarium* and allied fusarioid genera

R.C. Monteiro[1], C.Z. Yu[2], S. Dolatabadi[3], F. Hagen[4,5,6], M. Sandoval-Denis[4], P.W. Crous[4,7,8], M.C. Fisher[9], S.S. Gonçalves[10], Z.P. de Camargo[1], A.L. Hofling-Lima[2], A.M. Rodrigues[1,11]*

[1]Laboratory of Emerging Fungal Pathogens, Department of Microbiology, Immunology, and Parasitology, Discipline of Cellular Biology, Federal University of São Paulo (UNIFESP), São Paulo 04023062, Brazil
[2]Laboratory of Ophthalmology (LOFT), Department of Ophthalmology and Visual Sciences, Escola Paulista de Medicina (EPM), Federal University of São Paulo (UNIFESP), Sao Paulo 04023-062, Brazil
[3]Department of Biology, Hakim Sabzevari University, Sabzevar, Iran
[4]Westerdijk Fungal Biodiversity Institute, Uppsalalaan 8, 3584 CT Utrecht, The Netherlands
[5]Institute for Biodiversity and Ecosystem Dynamics, University of Amsterdam, Science Park 904, 1098 XH Amsterdam, The Netherlands
[6]Department of Medical Microbiology, University Medical Center Utrecht, Heidelberglaan 100, 3584 CX Utrecht, The Netherlands
[7]Department of Biochemistry, Genetics & Microbiology, Forestry & Agricultural Biotechnology Institute (FABI), University of Pretoria, Pretoria, South Africa
[8]Microbiology, Department of Biology, Utrecht University, Padualaan 8, Utrecht, 3584 CH, The Netherlands
[9]Medical Research Council Center for Global Infectious Disease Analysis, Department of Infectious Disease Epidemiology, School of Public Health, Imperial College London, London W2 1PG, UK
[10]Infectious Diseases Postgraduate Program, Center for Research in Medical Mycology, Federal University of Espírito Santo (UFES), Espírito Santo, 29043900, Brazil
[11]National Institute of Science and Technology in Human Pathogenic Fungi, Brazil

*Corresponding author: amrodrigues@unifesp.br / amrodrigues.amr@gmail.com

Key words:
AFLP
Bisifusarium
epidemiology
fusariosis
Fusarium
Neocosmospora

Abstract: Fusariosis is an emerging mycosis caused by diverse *Fusarium* and allied fusarioid genera that are characterized by spindle-shaped macroconidia. These fungi possess a broad ecological distribution, causing infections in a wide diversity of hosts, spanning the animal and plant kingdoms. The spectrum of human fusariosis encompasses superficial lesions like keratitis and onychomycosis to invasive fungal diseases. Notable genera within the medically relevant fusarioid group include *Neocosmospora*, *Fusarium s. str.*, and *Bisifusarium*. While *Neocosmospora* species (formerly *F. solani* species complex) are primary causative agents of human fusariosis, instances involving *Fusarium s. str.* and *Bisifusarium* (formerly *F. dimerum* species complex) have been reported. There is an urgent need for DNA-based markers to explore the epidemiology of these emerging fusarioid pathogens using molecular methods. We took advantage of fusarioid genomes available in NCBI (n = 20) to optimize the development of novel amplified fragment length polymorphism (AFLP) markers by conducting in-depth *in silico* analyses to refine their applicability for studies on these pathogens' genetic epidemiology. *In-silico* screening highlighted eight primer pair combinations (C1–C8) to be tested *in vitro*. The AFLP protocol was used for genotyping 40 medically relevant fusarioid fungi. Based on the overall scored AFLP markers (77–93 fragments), the values of polymorphism information content (*PIC* = 0.3474–0.3725), marker index (*MI* = 0.0038–0.0056), effective multiplex ratio (*E* = 26.3750–40.4750), resolving power (*Rp* = 40.1500–54.6000), discriminating power (*D* = 0.7978–0.8857), expected heterozygosity (*H* = 0.4476–0.4949), and mean heterozygosity (H_{ovp} = 0.0001) demonstrated the utility of these primer combinations for discriminating *Neocosmospora*, *Fusarium s. str.*, and *Bisifusarium* species. Of relevance, some AFLP panels were better than others at studying genetic trends in *Neocosmospora* (#2 EcoRI-AT/MseI-TA, #3 EcoRI-AA/MseI-TT, and #5 EcoRI-AT/MseI-AG) or *Fusarium s. str.* (mainly #2 EcoRI-AT/MseI-TA and #6 EcoRI-GA/MseI-TT) and *Bisifusarium* (#1 EcoRI-GA/MseI-AG and #6 EcoRI-GA/MseI-TT), and these combinations will better resolve disease transmission routes. Our DNA fingerprint assay has proven effective by exhibiting rapidity, reproducibility, and high discriminatory capabilities, which represents a valuable asset in the ongoing efforts to combat fusariosis and enhance our scientific understanding of medically relevant *Fusarium* and allied fusarioid genera.

Citation: Monteiro RC, Yu CZ, Dolatabadi S, Hagen F, Sandoval-Denis M, Crous PW, Fisher MC, Gonçalves SS, de Camargo ZP, Hofling-Lima AL, Rodrigues AM (2025). Novel amplified fragment length polymorphism (AFLP) markers for typing medically relevant *Fusarium* and allied fusarioid genera. *Fungal Systematics and Evolution* **15**: 79–96. doi: 10.3114/fuse.2025.15.03
Received: 23 June 2024; **Accepted:** 25 August 2024; **Effectively published online:** 2 October 2024
Corresponding editor: M. Arzanlou

Fungal Systematics and Evolution is licensed under a Creative Commons Attribution-NonCommercial-NoDerivatives 4.0 International License

© 2025 Westerdijk Fungal Biodiversity Institute

INTRODUCTION

Fusariosis is an emerging global mycosis caused by a group of fungi previously classified as *Fusarium sensu lato*. These fungi are characterized by their distinctive spindle-shaped macroconidia and are known to thrive in diverse environmental niches, infecting an extensive diversity of hosts spanning the animal, fungal, and plant kingdoms (Short *et al.* 2011, Bhunjun *et al.* 2024). Within the spectrum of human fusariosis, a wide range of manifestations exist, from relatively mild conditions like keratitis and onychomycosis (Milanez *et al.* 2024) to severe invasive fungal diseases that can affect multiple organs with sometimes fatal outcomes (Godoy *et al.* 2004, Nucci *et al.* 2013).

Medically relevant *Fusarium* and allied fusarioid genera constitute a composite of distinct fungi within the *Nectriaceae* family. *Bisifusarium*, *Neocosmospora*, and *Fusarium s. str.* are particularly noteworthy among these genera. *Neocosmospora* species, formerly known as the *F. solani* species complex (FSSC), have been recognized as primary causative agents of human fusariosis (Godoy *et al.* 2004, O'Donnell *et al.* 2016). However, there have also been documented cases of *Fusarium s. str.* (O'Donnell *et al.* 2004, Al-Hatmi *et al.* 2016a) and *Bisifusarium* (formerly the *F. dimerum* species complex) (Schroers *et al.* 2009) involvement in human patients.

Fusarioid fungi are significant in various contexts, ranking among the top 10 plant pathogens and contributing to grain toxin production (Wu 2007, Dean *et al.* 2012). Consequently, extensive research efforts in plant pathology have been dedicated to understanding these fungi, encompassing genetic methodologies to investigate their dissemination, epidemiology, population dynamics, and evolutionary trajectories (Zeller *et al.* 2003, Suga *et al.* 2004, Laraba *et al.* 2021). Nevertheless, specific genotyping methods developed for studying phytopathogenic fusarioid fungi may not be suitable for all medically relevant species.

In response to the need for robust genetic methods to study fusarioid fungi, researchers have employed Multilocus Sequence Typing (MLST), which involves the analysis of specific genes/loci to identify prevalent sequence types (ST) for epidemiological studies. Moreover, MLST has been essential in recognizing closely related species within *Neocosmospora* and *Fusarium s. str.* lineages. Additionally, it has aided in identifying genotypes closely associated with human fusariosis within the *F. oxysporum* species complex (FOSC) (Zhang *et al.* 2006, Edel-Hermann *et al.* 2016, Moretti *et al.* 2018).

However, while MLST is a robust approach, it is not without limitations, including high costs, time-intensive procedures, and labour requirements when compared to alternative DNA fingerprinting or Next-Generation Sequencing (NGS) methods (Bain *et al.* 2007, Jureen *et al.* 2008, O'Donnell *et al.* 2009, Chen *et al.* 2015). Identifying species and studying genetic variability within fusarioid fungi often requires analysing multiple genes, such as the translation elongation factor 1-alpha (*tef1α*) and the RNA polymerase second largest subunit (*rpb2*) (Debourgogne *et al.* 2010, Debourgogne *et al.* 2012). Alternatively, techniques that sample genome-wide Single Nucleotide Polymorphisms (SNPs) rather than the specific MLST loci have the potential to sample the genome more widely to facilitate understanding the genetic diversity within populations (Casanova *et al.* 2021, Qin *et al.* 2021). Nonetheless, only a few methods have been validated for such applications (Jureen *et al.* 2008, Silva *et al.* 2013). Notably, fingerprinting methods [microsatellite and variable-number tandem repeat (VNTR)] are not readily available for medically relevant fusarioid fungi.

The Amplified Fragment Length Polymorphism (AFLP) technique is widely employed for generating fingerprints of fusarioid fungi, serving as a valuable tool for conducting population-based genetic studies (de Oliveira Rocha *et al.* 2011, Barros *et al.* 2012). Despite the technique's demonstrated effectiveness in assessing variability within *Fusarium s. str.* and *Neocosmospora*, multiple AFLP schemes lack standardization or validation against quantitative metrics. A panel proposed by Leslie and Summerell has been developed, enabling the determination of fusarioid populations responsible for field-related diseases and the characterization of new species (Leslie & Summerell 2006, Barros *et al.* 2012). This AFLP scheme has subsequently found extensive application within phytopathological studies (Ramirez *et al.* 2007, Lee *et al.* 2009, Shiraishi *et al.* 2012). Additionally, commercial kits have been used for AFLP analyses (de Oliveira Rocha *et al.* 2011, Sharma *et al.* 2011). In human fusariosis, Al-Hatmi *et al.* (2016a, b) exploited AFLP analysis to investigate clinical *Fusarium* strains and described the features of *F. ficicrescens*. Interestingly, the same scheme has been applied to investigate *Fusarium* outbreaks, facilitating the tracking of clonal isolates for epidemiological investigations (Carlesse *et al.* 2017).

The primary limitations of AFLP arise from the arbitrary selection of selective bases (Vos *et al.* 1995), the dominant nature of the information, and the challenges associated with experimental reproducibility (Mueller & Wolfenbarger 1999). To overcome these problems, we took advantage of fusarioid genomic data available from NCBI datasets to optimize the technique for fusarioid species, strategically leveraging in-depth *in silico* analyses (de Carvalho *et al.* 2020). This optimization process fine-tuned the AFLP technique by targeting selective bases, enhancing its efficacy in addressing questions related to epidemiology, genetic diversity, and population structure within fusarioid species. We experimentally evaluated AFLP patterns upon refinement, enabling us to determine genetic relationships amongst species and characterize intraspecific diversity levels. Our study encompassed species implicated in outbreaks, notably *N. solani*. In a quest for finer-scale epidemiological insights, we conducted an exhaustive assessment of various primer combinations and identified the most effective panels to test epidemiological and evolutionary hypotheses.

MATERIALS AND METHODS

Fungal strains

Fungal samples were represented by 40 fusarioid strains (Table 1). Among these, 36 were recovered from ocular fusariosis specimens, including *Neocosmospora* (n = 24), *Fusarium* [n = 8; n = 6 comprising the FOSC, and n = 2 the *F. fujikuroi* species complex (FFSC)], and *Bisifusarium* (n = 4). The remaining four strains were obtained from environmental sources, with two each of *Neocosmospora* and *Fusarium* (FFSC). All fungi were maintained on malt extract agar (MEA) at room temperature.

DNA extraction and sequencing

Total DNA was obtained and purified directly from 7-d-old monoconidial colonies on potato dextrose agar (PDA) by the

© 2025 Westerdijk Fungal Biodiversity Institute

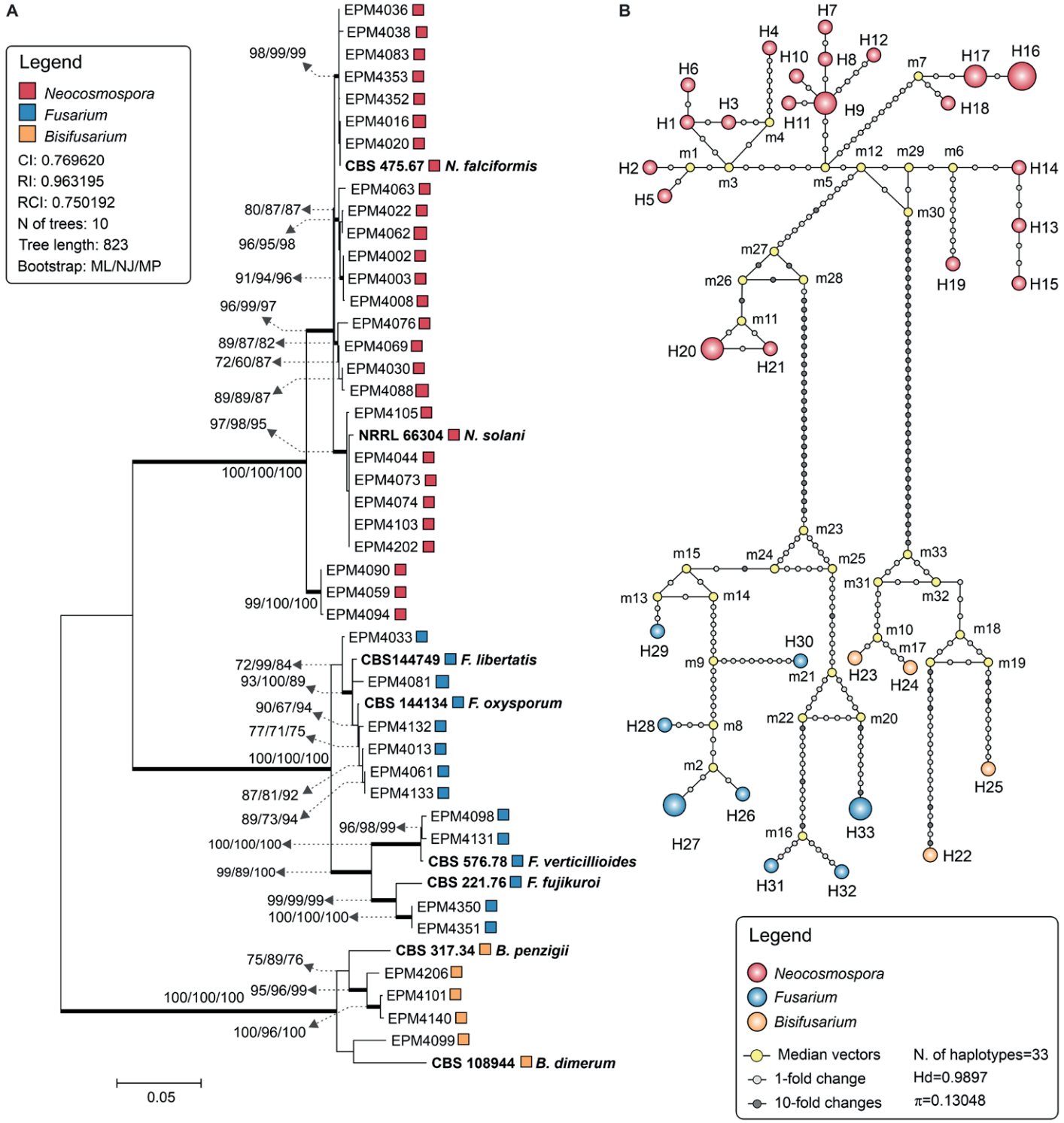


Fig. 1. Phylogenetic and haplotypic analysis based on partial sequence of *tef1α* and *rpb2*. **A.** Molecular identification was performed in the sequencing of *tef1α* and *rpb2*. Bold names refer to type strains. The phylogenetic tree was obtained in MEGA v. 7 using maximum likelihood, neighbour-joining, and maxima parsimony methods. Bootstrap values are reported in each branch. **B.** Haplotype network inferred by *tef1α* and *rpb2* sequences revealed 33 haplotypes (Hd = 0.9897, π = 0.13048).

FastDNA™ Kit protocol (MP Biomedical, Irvine, CA, USA), according to the manufacturer's recommendations. Samples were sequenced using primers EF1 (5' - ATG GGT AAG GAR GAC AAG AC-3') and EF2 (5' - GGA RGT ACC AGT SAT CAT GTT - 3') for *tef1α,* and 5f2 (5' - GGG GWG AYC AGA AGA AGG C-3') and 7cr (5' - CCC ATR GCT TGY TTR CCC AT - 3') for *rpb2* to identify the strains (O'Donnell *et al.* 1998, O'Donnell *et al.* 2007).

The PCR amplifications were performed using the PCR Master Mix (Promega, Madison, WI, USA) containing 0.05 U/ of *Taq* DNA Polymerase, 0.4 µM of each dNTP, 3 µM of $MgCl_2$, and 1 µM of each primer. Amplicons were purified using the Wizard® SV Gel and PCR Clean-Up System (Promega) as per manufacturer's recommendations. All cycling reactions were performed in a Mastercycler X50 (Eppendorf, Oslo, Norway).

Partial genes were sequenced in both directions, and a contig was assembled and analysed for each locus. Sequencing reactions were conducted in a Mastercycler X50 (Eppendorf) using a BigDye Terminator v. 3.1 Cycle Sequencing Kit (Applied Biosystems, Foster City, CA, USA), and the sequencing product was analysed in a SeqStudio Genetic Analyser (Applied Biosystems).

© 2025 Westerdijk Fungal Biodiversity Institute

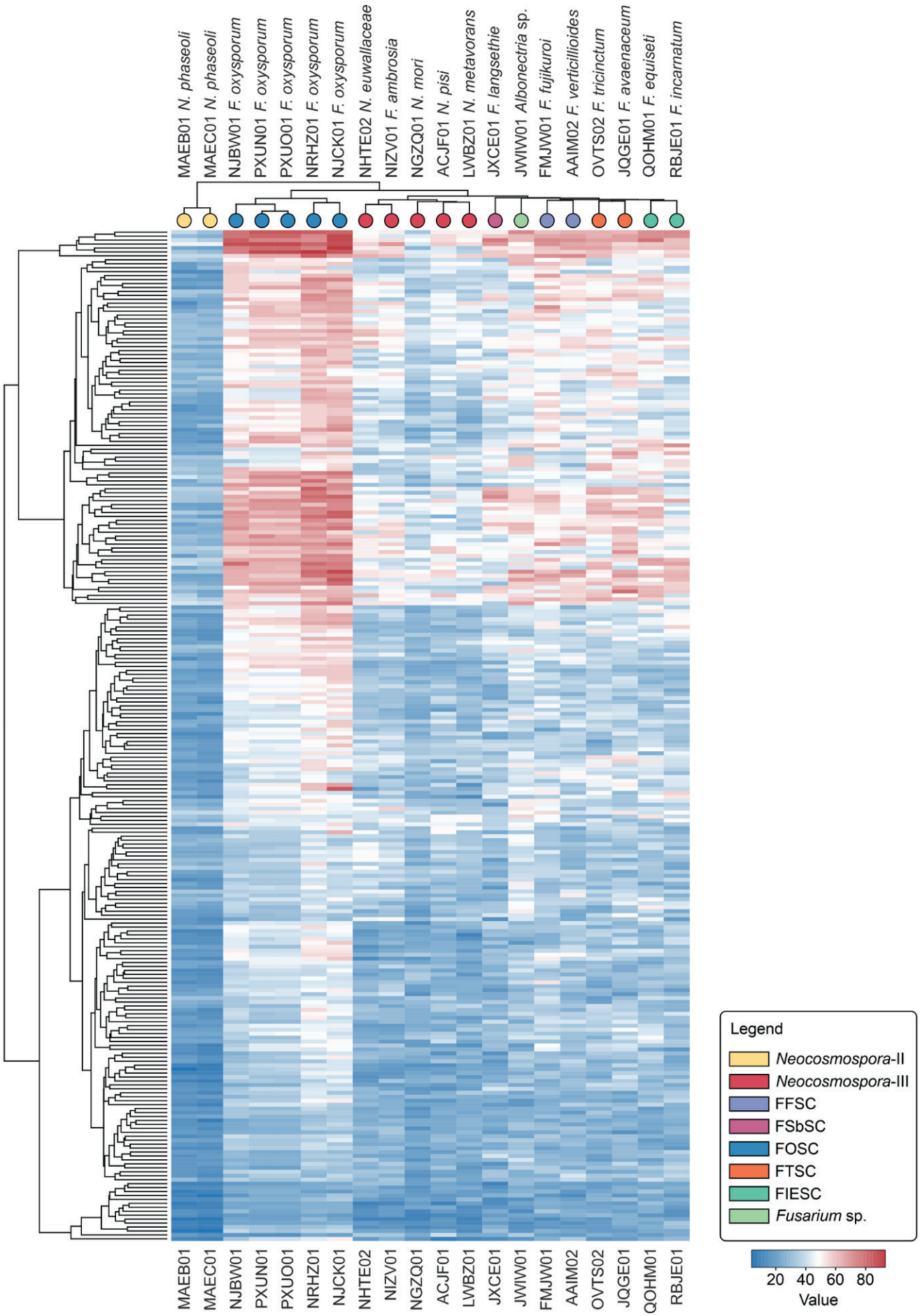


Fig. 2. Heatmap based on *in silico* AFLP profiles. A total of 256 combinations of selective primer pairs were tested *in silico* using 20 genomes of fusarioid retrieved from the NCBI GenBank Genome database, and 5 120 AFLP profiles were generated. The highest numbers of fragments are represented by red shading and the lower by blue shading.

© 2025 Westerdijk Fungal Biodiversity Institute

Mating type genotyping

Additionally, 50 ng of DNA samples were tested for mating type (*MAT*) using the type system developed by Kerényi *et al.* (2004). The primers fusALPHAfor (5' - CGC CCT CTK AAY GSC TTC ATG - 3'), and fusALPHArev (5' - GGA RTA RAC YTT AGC AAT YAG GGC - 3') for MAT 1-1, and fusHMGfor (5' - CGA CCT CCC AAY GCY TAC AT - 3'), and fusHMGrev (5' - TGG GCG GTA CTG GTA RTC RGG - 3') for MAT 1-2, were amplified separately and analysed with electrophoresis in a 1 % agarose gel (Sigma-Aldrich, St. Louis, MO, USA).

Molecular identification of fusaria

Phylogenetic inference based on concatenated partial *tef1α* and *rpb2* gene sequences was performed in MEGA v. 7 (Kumar *et al.* 2016) using neighbour-joining (NJ), maximum likelihood (ML), and maximum parsimony methods. Evolutionary distances were computed using the Kimura 2-parameters model (Kimura 1980) (for NJ and ML analyses) with 1 000 replicates of bootstrap resampling to assess branch robustness (Hillis & Bull 1993).

Nucleotide (π) and haplotype (Hd) diversities (Nei 1987) were calculated in DnaSP v. 6 (Rozas *et al.* 2017). A haplotype network was conducted using the median-joining method (Bandelt *et al.* 1999) in NETWORK v. 10.1 (Fluxus Technology, Suffolk, UK) to visualize genetics variabilities among the *Fusarium* species datasets. Sites containing gaps and missing data were not considered in the analysis.

In silico AFLP analyses

The *in silico* AFLP was performed as described by de Carvalho *et al.* (2020). Twenty whole-genome sequences of fusarioid species (Table 2) were analysed *in silico* to predict AFLP markers among the fusaria genomes. *In silico* AFLP analyses were performed using AFLPinSilico (Rombauts *et al.* 2003), and we considered fragment lengths from 50–600 bp. Firstly, *Fusarium* and allied genera genome sequences were collected from the NCBI GenBank Genome database and *in silico* digested with EcoRI and MseI restriction enzymes. Two hundred fifty-six combinations of two selective bases (EcoRI+NN and MseI+NN) were tested to track a subset of selective fragments. The number and size of the fragments were used to construct a matrix of fragments, and data were visualized using a heatmap. A hierarchical cluster analysis of *in silico* AFLP compositions was carried out using Heatmapper (Babicki *et al.* 2016), applying average linkage and Euclidean distance to each row cluster.

AFLP fingerprinting

AFLP *in vitro* experiments were conducted as described previously (Vos *et al.* 1995). In brief, 200 ng of genomic DNA was digested by EcoRI and MseI (New England Biolabs, Ipswich, MA, UK) and ligated to EcoRI and MseI adapters (Integrated DNA Technologies, San Diego, CA, USA). Preselective amplification was done using unlabelled EcoRI and MseI primers (Vos *et al.* 1995). Selective PCR was performed with EcoRI primers (5'-GAC TGC GTA CCA ATT CNN-3') and MseI primer (5'-GAT GAG TCC TGA GTA ANN-3'). EcoRI primers were fluorescent dye-labelled by 6-carboxyfluorescein (FAM; blue). Eight combinations of selective bases were chosen to test the potential as genetic markers for clinical fusarioid species (named combinations #1–8). The AFLP *in vitro* products were analysed by capillary gel electrophoresis in a SeqStudio Genetic Analyzer using LIZ600 as the internal size standard (Applied Biosystems). Each sample had at least two electropherograms imported to BioNumerics v. 7.6 (Applied Maths, St. Martens-Latem, Belgium) for each combination.

Fragments were automatically selected, considering only those robust and high-quality bands. Doubtful bands were excluded, setting a threshold at 100 relative fluorescent units (RFU), and only fragments with sizes between 50 and 600 base pairs were considered in BioNumerics v. 7.6. Positions for each band generated by selective amplification were converted to the binary matrix where presence (1) and absence (0) were indicated.

Relationships among fusarioid specimens were inferred using band-based Jaccard's similarity coefficient combined with a "fuzzy logic" method in BioNumerics v. 7.6. Dendrograms were obtained by the unweighted pair group mean arithmetic method (UPGMA). Branch faithfulness was assessed by cophenetic correlation coefficient calculation, and the standard derivation

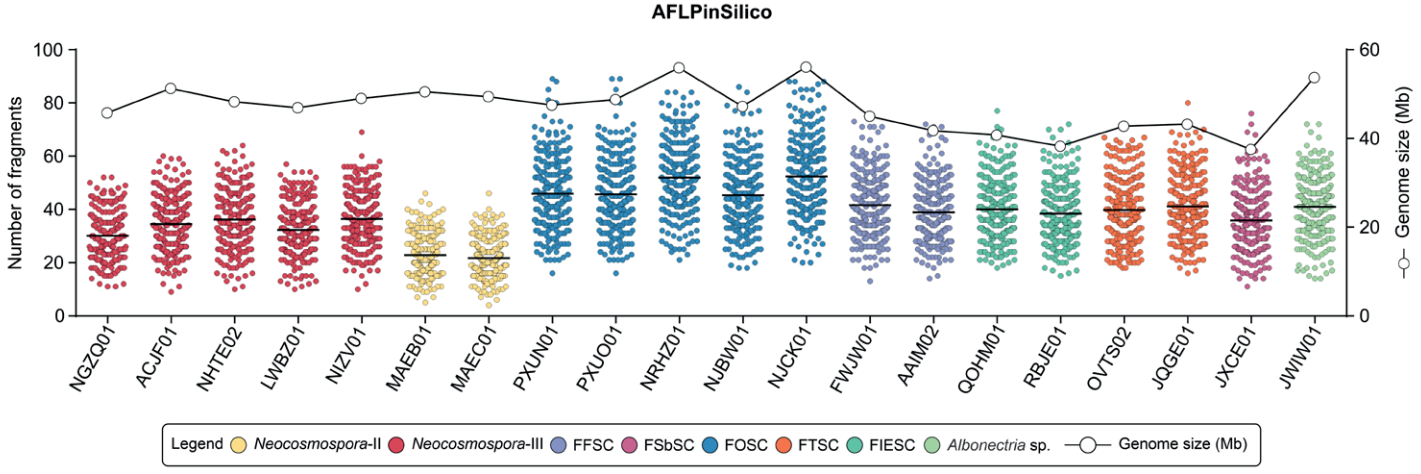


Fig. 3. Genome length and fragments amount from fusarioid species. The dots on the left X-axis represent the number of fragments generated for each combination (n = 256). The bold bar represents the average of fragments generated for all combinations. The white dots on the right X-axis represent the genome size, estimated by whole-genome sequencing.

© 2025 Westerdijk Fungal Biodiversity Institute

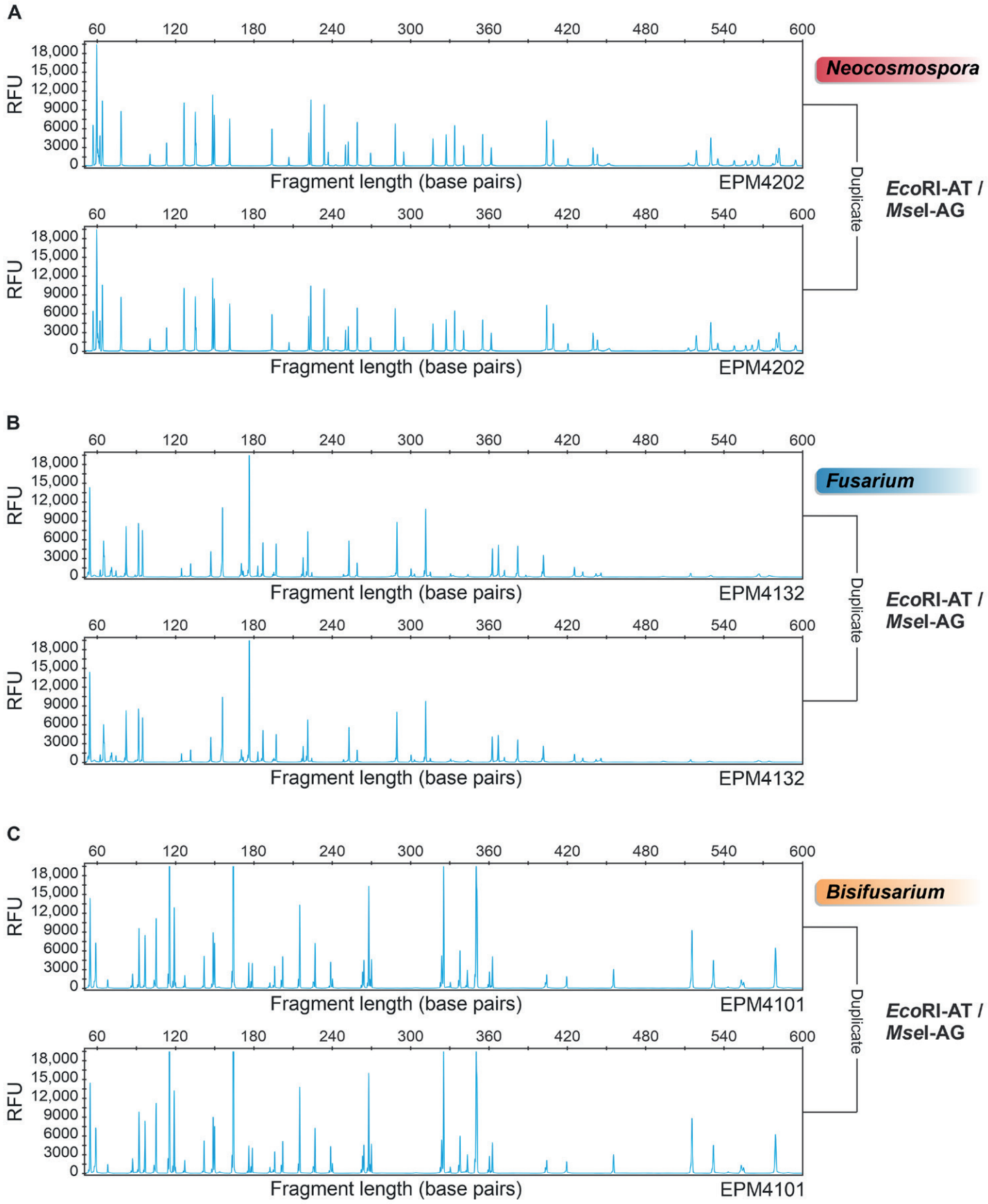


Fig. 4. Reproducibility of AFLP fingerprinting for *Neocosmospora*, *Fusarium*, and *Bisifusarium*. Electropherograms from fragment analysis performed in SeqStudio depicting the range of fragments between 50 and 600 bp for *Neocosmospora* EPM4202 (**A**), *Fusarium* EPM4132 (**B**), and *Bisifusarium* EPM4101 (**C**), with EcoRI-AT and MseI-AG selective primers labelled with blue (6-FAM). Error rates were never greater than 1.95 %, indicating that our protocol is highly reproducible.

© 2025 Westerdijk Fungal Biodiversity Institute

Table 1. Strains, species, source, origin, haplotypes, and GenBank accession numbers of fusarioid isolates used in this study.

Isolate code	Species		Source	Origin	Mating type	*tef1α*	*rpb2*
EPM4101	*Bisifusarium*	*delphinoides*	Keratitis	Brazil	*MAT1-1*	PP934305	PP934345
EPM4140		*delphinoides*	Keratitis	Brazil	*MAT1-1*	PP934311	PP934351
EPM4099		sp. FDSC-clade I	Keratitis	Brazil	*MAT1-1*	PP934304	PP934344
EPM4206		sp. FDSC-clade III	Keratitis	Brazil	*MAT1-1*	PP934313	PP934353
EPM4350	*Fusarium*	*annulatum*	Environment	Iran	*MAT1-2*	PP934314	PP934354
EPM4351		*annulatum*	Environment	Iran	*MAT1-2*	PP934315	PP934355
EPM4013		*contaminatum*	Keratitis	Brazil	*MAT1-2*	PP934281	PP934321
EPM4132		*curvatum*	Keratitis	Brazil	*MAT1-2*	PP934309	PP934349
EPM4033		sp. FOSC-clade I	Keratitis	Brazil	*MAT1-1*	PP934286	PP934326
EPM4081		sp. FOSC-clade III	Keratitis	Brazil	*MAT1-2*	PP934298	PP934338
EPM4098		*verticillioides*	Keratitis	Brazil	*MAT1-1*	PP934303	PP934343
EPM4131		*verticillioides*	Keratitis	Brazil	*MAT1-2*	PP934308	PP934348
EPM4133		*veterinarium*	Keratitis	Brazil	*MAT1-1*	PP934310	PP934350
EPM4061		*veterinarium*	Keratitis	Brazil	*MAT1-1*	PP934291	PP934331
EPM4352	*Neocosmospora*	*falciformis*	Environment	Iran	*MAT1-1*	PP934316	PP934356
EPM4353		*falciformis*	Environment	Iran	*MAT1-1*	PP934317	PP934357
EPM4038		*falciformis*	Keratitis	Brazil	*MAT1-1*	PP934288	PP934328
EPM4016		*falciformis*	Keratitis	Brazil	*MAT1-1*	PP934282	PP934322
EPM4020		*falciformis*	Keratitis	Brazil	*MAT1-1*	PP934283	PP934323
EPM4036		*falciformis*	Keratitis	Brazil	*MAT1-2*	PP934287	PP934327
EPM4083		*falciformis*	Keratitis	Brazil	*MAT1-1*	PP934299	PP934339
EPM4002		*keratoplastica*	Keratitis	Brazil	*MAT1-1*	PP934278	PP934318
EPM4003		*keratoplastica*	Keratitis	Brazil	*MAT1-1*	PP934279	PP934319
EPM4008		*keratoplastica*	Keratitis	Brazil	*MAT1-1*	PP934280	PP934320
EPM4022		*keratoplastica*	Keratitis	Brazil	*MAT1-2*	PP934284	PP934324
EPM4062		*keratoplastica*	Keratitis	Brazil	*MAT1-1*	PP934292	PP934332
EPM4063		*keratoplastica*	Keratitis	Brazil	*MAT1-1*	PP934293	PP934333
EPM4090		*petroliphila*	Keratitis	Brazil	*MAT1-1*	PP934301	PP934341
EPM4094		*petroliphila*	Keratitis	Brazil	*MAT1-2*	PP934302	PP934342
EPM4059		*petroliphila*	Keratitis	Brazil	*MAT1-2*	PP934290	PP934330
EPM4074		*solani*	Keratitis	Brazil	*MAT1-2*	PP934296	PP934336
EPM4044		*solani*	Keratitis	Brazil	*MAT1-2*	PP934289	PP934329
EPM4073		*solani*	Keratitis	Brazil	*MAT1-2*	PP934295	PP934335
EPM4103		*solani*	Keratitis	Brazil	*MAT1-1*	PP934306	PP934346
EPM4105		*solani*	Keratitis	Brazil	*MAT1-2*	PP934307	PP934347
EPM4202		*solani*	Keratitis	Brazil	*MAT1-2*	PP934312	PP934352
EPM4030		*suttoniana*	Keratitis	Brazil	*MAT1-1*	PP934285	PP934325
EPM4069		*suttoniana*	Keratitis	Brazil	*MAT1-2*	PP934294	PP934334
EPM4076		*suttoniana*	Keratitis	Brazil	*MAT1-2*	PP934297	PP934337
EPM4088		*suttoniana*	Keratitis	Brazil	*MAT1-2*	PP934300	PP934340

was used to express the consistency of a given cluster, which determines the correlation between the dendrogram-derived similarities and the matrix similarities, as described by de Carvalho *et al.* (2020).

Topological congruence between any two AFLP dendrograms or each AFLP dendrogram and phylogenetic trees was tested using the maximum agreement subtrees (MAST) with congruence index (I_{cong}) calculated from Newick files (de Vienne *et al.* 2007). Additionally, similarity matrixes were compared using the Mantel test (Mantel 1967) to reveal a correlation between AFLP dendrograms and phylogenetic trees using the package Vegan in R v. 4.0.3 (Oksanen *et al.* 2019). The sequencing-based p-distance was calculated in MEGA v. 7 using the Kimura 2-parameters model (Kimura 1980, Kumar *et al.* 2016). Finally, experiment congruence analysis between AFLP was performed in BioNumerics v. 7.6 (Applied Maths).

The genetic relationship among fusarioid specimens was evaluated using the minimum spanning tree (MST) model based

© 2025 Westerdijk Fungal Biodiversity Institute

on AFLP band profiles, performed in BioNumerics v. 7.6. In the MST model, in a set of distances, the minimum spanning tree that connects all samples is given by the shortest possible value of the summed distance of all branches (Kimura 1980). All analysis reports were exported and treated using Corel Draw 2019 (Corel, Ottawa, Canada).

Reproducibility of AFLP markers

Each sample had two independent replicates of all *in vitro* AFLP procedures to evaluate the reproducibility of AFLP fragment profiles (Bonin *et al.* 2004). A single error rate was calculated for all samples based on the percentage of mismatched loci between the replicate pairs (Pompanon *et al.* 2005).

Genetic diversity and statistical analysis

To assess which combinations of selective primers were the most informative, the following polymorphism indices were calculated using iMEC (Amiryousefi *et al.* 2018): polymorphic information content (*PIC*) (Botstein *et al.* 1980), expected heterozygosity (*H*) (Liu 1998), effective multiplex ratio (*E*) (Powell *et al.* 1996), arithmetic mean heterozygosity (H_{avp}) (Powell *et al.* 1996), marker index (*MI*) (Powell *et al.* 1996, Varshney *et al.* 2007), discriminating power (*D*) (Tessier *et al.* 1999), and resolving power (*Rp*) (Prevost & Wilkinson 1999).

Dimensioning analysis

Based on automated band matching, a principal component analysis (PCA) was carried out to produce three-dimensional plots in BioNumerics v. 7.6. Automated band matching was performed in all samples considering minimum profiling of 5 %, with the optimization and position tolerances set to 0.10 % for generated bands. A PCA was generated by subtracting the average for characters (Rodrigues *et al.* 2020).

RESULTS

Forty representatives of fusarioid fungi were included in our study, and all specimens of clinical origin were obtained from cases of ocular fusariosis. *Neocosmospora* specimens (n = 26) (formally FSSC) were composed of *N. solani* (n = 6), *N. keratoplastica* (n = 6), *N. suttoniana* (n = 4), *N. petroliphila* (n = 1), and *N. falciformis* (n = 7; including two environmental isolates). In *Fusarium* spp., FOSC members (n = 6) were composed of strains from clades I (n = 1), II (n = 1), VII (n = 3), and VIII (n = 1) that bear clinically relevant species, and for FFSC, two samples of *F. verticillioides* (clinical samples) and *F. annulatum* (environmental source) were included. Finally, *Bisifusarium* (n = 4) (formally FDSC) was represented by clades I (n = 1) and II (n = 3) (Table 1), known to be clinically relevant (Salah *et al.* 2015, van Diepeningen *et al.* 2015).

Concatenated *tef1α* and *rpb2* sequences were 1 585 bp long and had 487 (30.72 %) polymorphic sites comprising 33 (2.08 %) singletons and 454 (28.64 %) parsimony informative sites. All species complexes in this study were supported by high bootstrap values (100 %) (Fig. 1). The total number of mutations of 115 conferred a moderate nucleotide diversity (π) for *Neocosmospora* (π = 0.016), while both *Fusarium* (π = 0.044, 156 mutations) and *Bisifusarium* (π = 0.050, 177 mutations) were more diverse. Haplotype diversity based on *tef1α* and *rpb2* partial sequences revealed the highest diversity among samples

Table 2. Genomes of *Fusarium* and allied fusarioid genera retrieved from the NCBI Genome database for *in silico* analysis.

Species	Clade/Species complex	Strain	Access	Length (Mb)	Contigs	Reference
Neocosmospora mori	*Neocosmospora* - clade 3	JS-169	NGZQ01	45.80	7 631	Al-Reedy *et al.* (2012)
N. pisi	*Neocosmospora* - clade 3	77-13-4	ACJF01	51.30	8 759	Coleman *et al.* (2009)
N. euwallaceae	*Neocosmospora* - clade 3	HFEW-16-IV-019	NHTE02	48.31	9 18	Sayers *et al.* (2022)
N. metavorans	*Neocosmospora* - clade 3	MYA-4552	LWBZ01	46.90	8 182	Herr *et al.* (2016)
N. ambrosia	*Neocosmospora* - clade 3	NRRL 20438	NIZV01	49.00	9 241	Xie *et al.* (2022)
N. phaseoli	*Neocosmospora* - clade 2	NRRL 31156	MAEB01	50.50	11 647	Huang *et al.* (2016)
F. brasiliense	*Neocosmospora* - clade 2	NRRL 31757	MAEC01	49.40	11 591	Huang *et al.* (2016)
F. oxysporum s. l.	FOSC	VEG-01C2	PXUN01	47.50	13 172	Sayers *et al.* (2022)
F. oxysporum s. l.	FOSC	VEG-01C1	PXUO01	48.80	11 487	Sayers *et al.* (2022)
F. oxysporum f. sp. conglutinans	FOSC	58385	NRHZ01	55.90	13 297	Liu *et al.* (2019)
F. oxysporum s. l.	FOSC	KOD886	NJBW01	47.20	10 554	van Dam *et al.* (2018)
F. oxysporum f. sp. gladioli	FOSC	G76	NJCK01	56.10	9 875	van Dam & Rep (2017)
F. fujikuroi	FFSC	MRC2276	FMJW01	45.00	10 394	Niehaus *et al.* (2017)
F. verticillioides	FFSC	7600	AAIM02	41.80	9 076	Cuomo *et al.* (2007)
F. equiseti	FIESC	D25-1	QOHM01	40.80	5 805	Sayers *et al.* (2022)
F. incarnatum	FIESC	MOD1-FUNGI17	RBJE01	38.30	5 513	Sayers *et al.* (2022)
F. tricinctum	FTSC	INRA104	OVTS02	42.80	10 079	Ponts *et al.* (2020)
F. avenaceum	FTSC	FaLH27	JQGE01	43.20	10 164	Lysøe *et al.* (2014)
F. langsethiae	FSBSC	Fl201059	JXCE01	37.50	9 756	Lysøe *et al.* (2016)
Albonectria sp.	Unknown	JS1030	JWIW01	53.70	10 412	Li *et al.* (2021)

© 2025 Westerdijk Fungal Biodiversity Institute

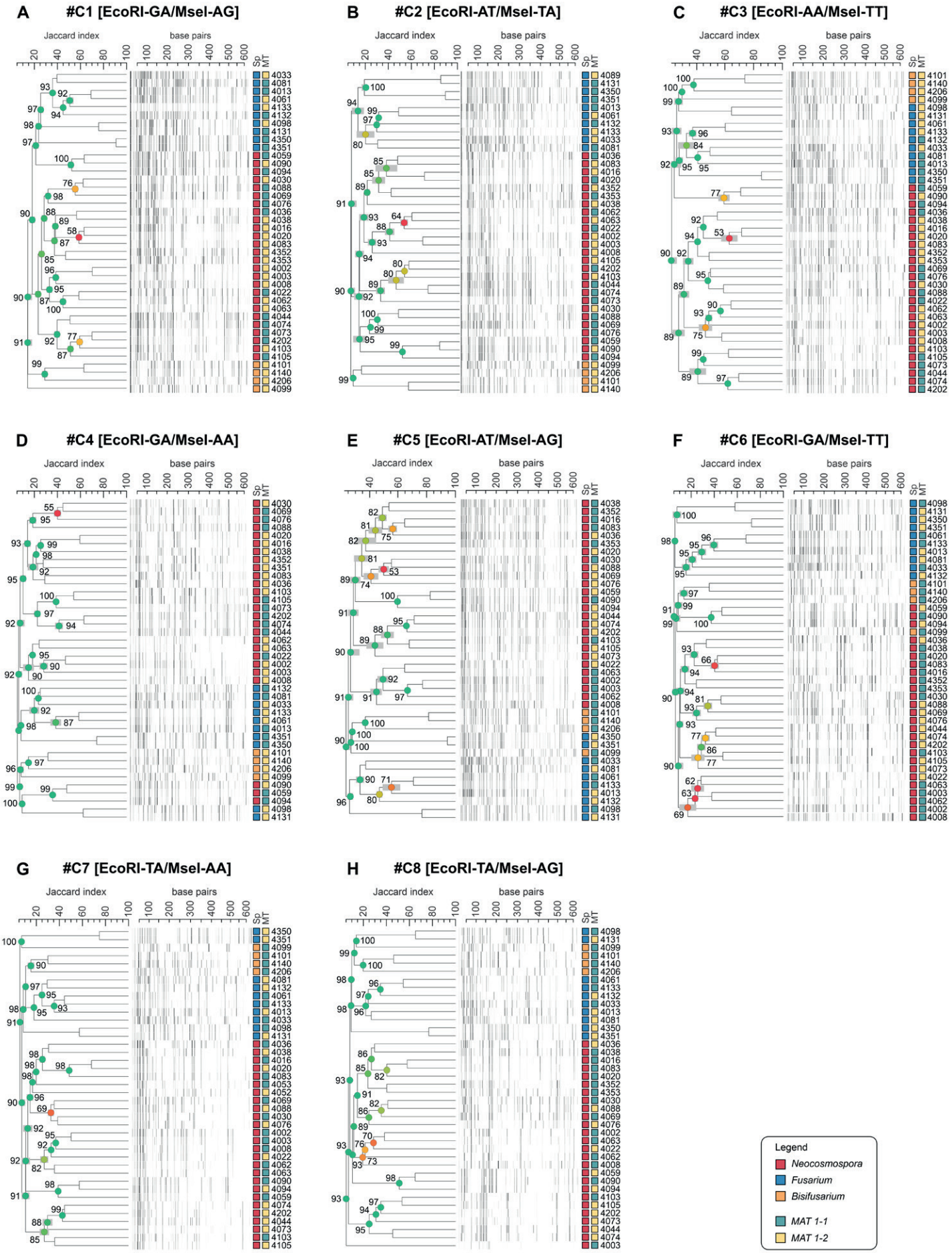


Fig. 5. UPGMA clustering based on AFLP from C1 to C8 (**A–H**, respectively). Markers were used to compute a similarity matrix using the Jaccard index and the "fuzzy logic" method. UPGMA rendered a highly supported cophenetic values tree for each combination. Sp = species; *MAT* = mating type.

© 2025 Westerdijk Fungal Biodiversity Institute

within 33 haplotypes (Hd = 0.99, π = 0.130) (Fig. 1).

In our efforts to create AFLP markers for exploring the diversity within clinically significant fusarioid species, we first retrieved the genomes of these fungi from NCBI (Table 2). Then, we conducted an *in silico* digestion using AFLPinSilico. Afterward, the genomes were mined using 256 combinations of two selective bases for EcoRI+NN and MseI+NN primers. This process generated a fragment matrix containing 5 120 AFLP profiles (Fig. 2). The fragments ranged from 4 to 93, with no observed correlation with genome size (Pearson correlation r = 0.2117, p = 0.3702) (Fig. 3).

The heatmap showed two large clusters, one with the highest number of fragments and the other with the lowest values (Fig. 2). Our selection criteria aimed to strike a balance, preferring combinations that would not lead to size homoplasy fragments and would effectively highlight the distinctions among the studied genomes. As a result, we chose eight candidate combinations (#1–8) for further experimental testing.

The eight combinations explored variability among 90–93 loci (93 for #1 and #2, 85 for #3, 84 for #4, 90 for #5, 78 for #6 and #7, and 77 for #8). For *Neocosmospora*, a polymorphic number of fragments ranged from 71 to 90, while *Fusarium* ranged from 62 to 83. The number of fragments for *Bisifusarium* varied between 50 and 69 fragments. Table 3 shows all parameters of diversity studied here.

Expected heterozygosity (*H*) or haplotype diversity was calculated, and values ranged from 0.45–0.49. Haplotype diversity is an index that predicts the proportion of heterozygous genotypes or different haplotypes expected under the Hardy-Weinberg equilibrium. All markers reported good *H* values

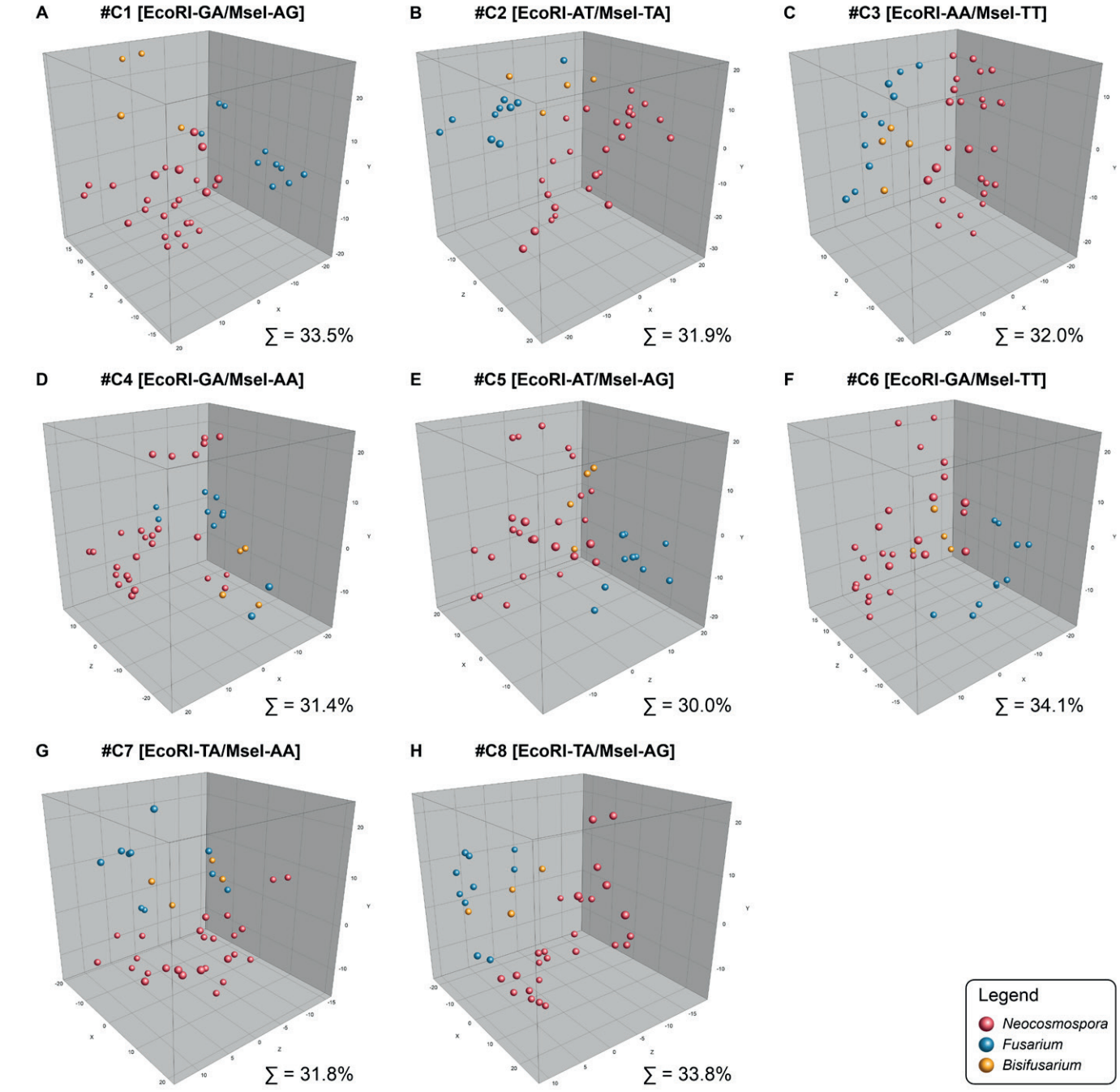


Fig. 6. Principal component analysis (PCA) built using AFLP fingerprinting. PCA of combinations 1 to 8 (**A–H**, respectively). PCAs were constructed using BioNumerics v. 7.6. The PCAs were used to demonstrate the correlations among the 40 samples of fusarioid using the eight primer pair combinations. Coloured spheres represent the strains.

© 2025 Westerdijk Fungal Biodiversity Institute

Table 3. Diversity indices calculated from AFLP fingerprinting *in vitro*.

#1 EcoRI-GA/MseI-AG									
Species	**Scored bands**	***H***	***PIC***	***E***	H_{avp}	***MI***	***D***	***Rp***	**Error %**
Neocosmospora	90	0.4822	0.3659	365.000	0.0002	0.0075	0.8356	443.846	1.15
Fusarium	83	0.4862	0.3680	484.000	0.0006	0.0284	0.6602	400.000	1.27
Bisifusarium	64	0.4878	0.3688	370.000	0.0019	0.0705	0.6667	380.000	1.56
Overall	93	0.4910	0.3704	402.500	0.0001	0.0053	0.8128	546.000	1.18
#2 EcoRI-AT/MseI-TA									
Species	**Scored bands**	***H***	***PIC***	***E***	H_{avp}	***MI***	***D***	***Rp***	**Error %**
Neocosmospora	88	0.4946	0.3723	394.231	0.0002	0.0085	0.7994	488.462	0.93
Fusarium	77	0.4887	0.3693	443.000	0.0006	0.0281	0.6693	426.000	1.52
Bisifusarium	69	0.4979	0.3739	367.500	0.0018	0.0663	0.7172	385.000	1.45
Overall	93	0.4910	0.3704	402.500	0.0001	0.0053	0.8128	546.000	1.08
#3 EcoRI-AA/MseI-TT									
Species	**Scored bands**	***H***	***PIC***	***E***	H_{avp}	***MI***	***D***	***Rp***	**Error %**
Neocosmospora	78	0.4819	0.3658	315.769	0.0002	0.0075	0.8362	400.769	1.04
Fusarium	75	0.4991	0.3745	359.000	0.0007	0.0239	0.7712	366.000	1.02
Bisifusarium	65	0.4595	0.3539	417.500	0.0018	0.0738	0.5883	335.000	1.15
Overall	85	0.4795	0.3646	339.000	0.0001	0.0048	0.8410	465.000	1.47
#4 EcoRI-GA/MseI-AA									
Species	**Scored bands**	***H***	***PIC***	***E***	H_{avp}	***MI***	***D***	***Rp***	**Error %**
Neocosmospora	84	0.4618	0.3551	303.846	0.0002	0.0064	0.8693	438.462	0.97
Fusarium	72	0.4999	0.3749	354.000	0.0007	0.0246	0.7586	440.000	0.69
Bisifusarium	58	0.4955	0.3727	317.500	0.0021	0.0678	0.7014	335.000	1.29
Overall	84	0.4688	0.3589	315.000	0.0001	0.0044	0.8594	486.000	1.49
#5 EcoRI-AT/MseI-AG									
Species	**Scored bands**	***H***	***PIC***	***E***	H_{avp}	***MI***	***D***	***Rp***	**Error %**
Neocosmospora	88	0.4986	0.3743	416.538	0.0002	0.0091	0.7761	491.538	1.05
Fusarium	76	0.4999	0.3750	376.000	0.0007	0.0247	0.7556	376.000	0.92
Bisifusarium	70	0.4814	0.3655	417.500	0.0017	0.0718	0.6451	385.000	1.07
Overall	90	0.4949	0.3725	404.750	0.0001	0.0056	0.7978	519.500	1.61
#6 EcoRI-GA/MseI-TT									
Species	**Scored bands**	***H***	***PIC***	***E***	H_{avp}	***MI***	***D***	***Rp***	**Error %**
Neocosmospora	81	0.4318	0.3386	255.385	0.0002	0.0052	0.9007	396.923	1.37
Fusarium	62	0.4996	0.3748	301.000	0.0008	0.0243	0.7647	334.000	0.55
Bisifusarium	47	0.4991	0.3745	245.000	0.0027	0.0650	0.7296	250.000	1.06
Overall	78	0.4476	0.3474	263.750	0.0001	0.0038	0.8857	423.500	1.79
#7 EcoRI-TA/MseI-AA									
Species	**Scored bands**	***H***	***PIC***	***E***	H_{avp}	***MI***	***D***	***Rp***	**Error %**
Neocosmospora	72	0.4649	0.3568	264.615	0.0002	0.0066	0.8651	338.462	1.13
Fusarium	71	0.4964	0.3732	325.000	0.0007	0.0227	0.7908	374.000	1.02
Bisifusarium	56	0.4885	0.3692	322.500	0.0022	0.0703	0.6694	325.000	1.34
Overall	78	0.4632	0.3559	284.250	0.0001	0.0042	0.8673	401.500	1.67
#8 EcoRI-TA/MseI-AG									
Species	**Scored bands**	***H***	***PIC***	***E***	H_{avp}	***MI***	***D***	***Rp***	**Error %**
Neocosmospora	71	0.4582	0.3532	252.308	0.0002	0.0063	0.8738	381.539	1.72
Fusarium	63	0.4990	0.3745	301.000	0.0008	0.0238	0.7721	354.000	1.03
Bisifusarium	56	0.4960	0.3730	305.000	0.0022	0.0675	0.7045	320.000	1.34
Overall	77	0.4550	0.3515	269.500	0.0001	0.0040	0.8776	423.000	1.95

D = discriminating power; *E* = effective multiplex ratio; *H* = expected heterozygosity; H_{avp} = mean heterozygosity; *MI* = marker index; *PIC* = polymorphism information content; *Rp* = resolving power.

© 2025 Westerdijk Fungal Biodiversity Institute

except combination #7 for FFSC, with a shallow *H* value of 0.0921, indicating that no haplotype diversity could be identified using that AFLP marker (Table 3).

We assessed the polymorphism information content (*PIC*) for each AFLP marker, revealing excellent values. Specifically, combinations #5, #1, and #2 exhibited the highest *PIC* values at 0.37. *Neocosmospora* displayed interesting *PIC* values within the genus, with combinations #5 and #2 emerging as the most suitable options for investigating variability. On the other hand, all combinations yielded *PIC* values ≥ 0.37 for *Fusarium*, except for combination #3, which was not as effective for studying diversity in *Bisifusarium* (Table 3).

The marker index (*MI*) helps estimate the total utility of the maker system, while resolving power (*Rp*) is a parameter used to calculate a marker to detect differences between more significant numbers of genotypes. The *MI* ranged from 0.0039 to 0.0056 for overall markers. Combinations #5 (0.0056), #1 (0.0053), and #2 (0.0053) obtained the highest values. The *Rp* has the lowest value in combination #7 at 40.15 and its highest value in combination #1 and #2 at 54.60. Both can be considered good *Rp* values, but *Rp* between the specimens had medium values of 40.21 and 41.10 for combination #1 and #2, respectively, while combination #7 had medium values of 24.42. From this assessment, combinations #1, #2, and #5 are the most informative among the markers (Table 3).

Related to *MI* and *Rp*, effective multiplex ratio (*E*) calculated the information generated from polymorphic loci in the marker system and varied from 26.37–40.48 overall markers. Markers #1, #2, and #5 had the highest values. Discriminating power (*D*) is a helpful statistical parameter to indicate the probability that two individuals, taken randomized, exhibit different genotypes using a marker system. *D*-values varied between 0.80 for combination #5 and 0.89 for combination #6, indicating that all markers efficiently study diversity in a fusarioid of clinical interest (Table 3).

The electropherograms of fusarioid AFLP (ranging from 50 to 600 bp) demonstrated high reproducibility for each of the studied species, including those belonging to *Neocosmospora* (Fig. 4A), *Fusarium* (Fig. 4B), and *Bisifusarium* (Fig. 4C). Furthermore, acceptable error rates typically fall within 2 % to

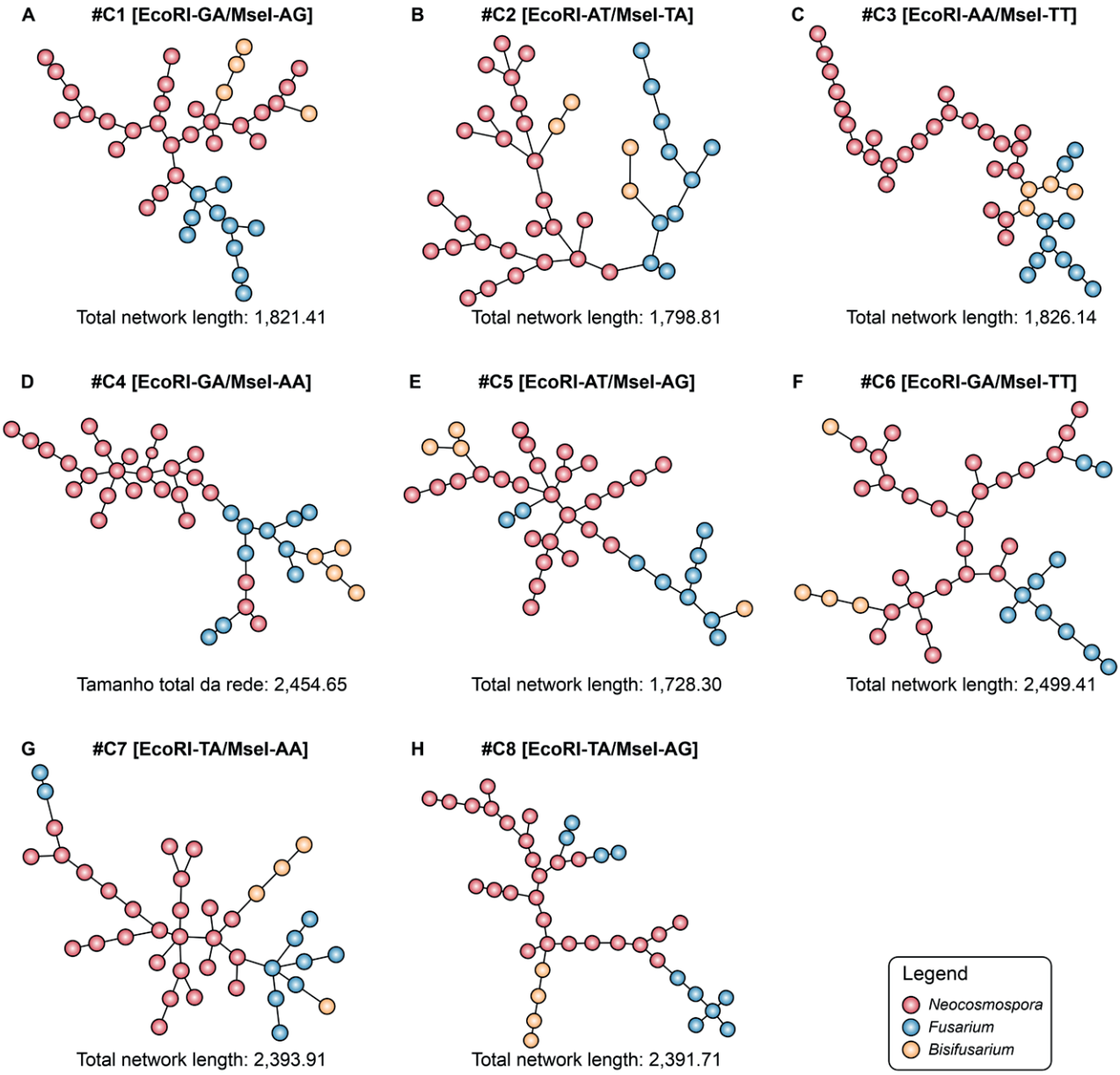


Fig. 7. A minimal spanning tree (MST) was built using AFLP fingerprinting. AFLP-derived MSTs of fusarioid using combinations 1 to 8 (**A–H**, respectively). These MSTs highlighted different genetic variants since the finer resolution was obtained using AFLP markers.

© 2025 Westerdijk Fungal Biodiversity Institute

Table 4. Comparison among the congruent clustering methods used for phylogenetic analysis and AFLP-derived dendrograms for combinations #1 to #8 generated by congruence index values (I_{cong}).

Comparison	I_{cong}	*p*-value	Leaves	MAST
AFLP1 *vs*. AFLP2	162.156	0.00003	40	15
AFLP1 *vs*. AFLP3	227.019	0.00000	40	21
AFLP1 *vs*. AFLP4	151.346	0.00021	40	14
AFLP1 *vs*. AFLP5	183.777	0.00000	40	17
AFLP1 *vs*. AFLP6	151.346	0.00021	40	14
AFLP1 *vs*. AFLP7	183.777	0.00000	40	17
AFLP1 *vs*. AFLP8	194.587	0.00000	40	18
AFLP2 *vs*. AFLP3	216.208	0.00000	40	20
AFLP2 *vs*. AFLP4	140.535	0.00137	40	13
AFLP2 *vs*. AFLP5	140.535	0.00137	40	13
AFLP2 *vs*. AFLP6	172.967	0.00000	40	18
AFLP2 *vs*. AFLP7	194.587	0.00000	40	12
AFLP2 *vs*. AFLP8	172.967	0.00000	40	18
AFLP3 *vs*. AFLP4	162.156	0.00003	40	15
AFLP3 *vs*. AFLP5	205.398	0.00000	40	19
AFLP3 *vs*. AFLP6	183.777	0.00000	40	17
AFLP3 *vs*. AFLP7	248.639	0.00000	40	23
AFLP3 *vs*. AFLP8	227.019	0.00000	40	21
AFLP4 *vs*. AFLP5	140.535	0.00137	40	13
AFLP4 *vs*. AFLP6	140.535	0.00137	40	13
AFLP4 *vs*. AFLP7	172.967	0.00000	40	16
AFLP4 *vs*. AFLP8	129.725	0.00897	40	12
AFLP5 *vs*. AFLP6	172.967	0.00000	40	16
AFLP5 *vs*. AFLP7	194.587	0.00000	40	18
AFLP5 *vs*. AFLP8	172.967	0.00000	40	18
AFLP6 *vs*. AFLP7	194.587	0.00000	40	18
AFLP6 *vs*. AFLP8	172.967	0.00000	40	16
AFLP7 *vs*. AFLP8	227.019	0.00000	40	21
AFLP1 *vs*. Sequencing	140.535	0.00137	40	13
AFLP2 *vs*. Sequencing	162.156	0.00003	40	15
AFLP3 *vs*. Sequencing	140.535	0.00137	40	13
AFLP4 *vs*. Sequencing	118.915	0.05852	40	11
AFLP5 *vs*. Sequencing	140.535	0.00137	40	13
AFLP6 *vs*. Sequencing	183.777	0.00000	40	17
AFLP7 *vs*. Sequencing	151.346	0.00021	40	14
AFLP8 *vs*. Sequencing	216.208	0.00000	40	20

5 % (Bonin *et al.* 2004, Pompanon *et al.* 2005). In our analysis of fusarioid AFLP markers, we observed an average error rate varying from 1.08 % to 1.95 %. Specifically, *Neocosmospora* exhibited error rates between 0.93 % and 1.72 %, *Fusarium* rates ranged from 0.55 % to 1.27 %, and *Bisifusarium* had rates from 1.06 % to 1.56 % (Table 3). Details of these indices computed separately for each species or species complex are available in Supplementary Table S1.

Cluster analysis of the AFLP profiles, as depicted in Fig. 5, resulted in well-supported dendrograms, with most cophenetic values exceeding 90 %. The similarity values among all combinations ranged from 10.89 % to 91.45 %, with a median value of 30.35 % ± 12.90 %. Details of the similarity values for each combination are shown in Supplementary Table S2. Interestingly, the similarity values among combinations strongly correlated with each other in the Mantel test. However, they showed only a moderate correlation with the *p*-distance based on sequencing, as illustrated in Supplementary Fig. S1 and Supplementary Table S3.

Although correlation values were lower than those observed in the Mantel test, a similar result was observed in the experiment congruence analysis performed in BioNumerics v. 7.6 (Supplementary Fig. S2, Supplementary Table S4). This difference could be due to Mantel test analyses adopting a randomization or permutation test accessing an elevated correlation coefficient (Mantel 1967, Diniz-Filho *et al.* 2013). Also, experiment congruence reveals that combinations #1 and #6 have similar performance, as well as combinations #5 and #2 (Supplementary Fig. S2, Supplementary Table S4).

These findings suggest that certain AFLP markers may be more suitable for distinguishing specific genera of fusarioid fungi, while others may not be as effective. However, it is important to note that genetic history can still be reconstructed using any tested AFLP markers or through sequencing, and the AFLP dendrograms/phylogenetic trees we derived are highly consistent (Table 4).

Overall, *Neocosmospora*, including *N. solani*, *N. falciformis*, *N. keratoplastica*, and *N. suttoniana*, presented a similar clustering in all AFLP markers. However, *N. petroliphila* is sometimes included in or out of the *Neocosmospora* clade, suffering from incongruence. Moreover, *N. petroliphila* is less genetically related to the other clinical samples included in this study based on sequencing. Also, a *Fusarium* clade (composed of FOSC and FFSC) was observed in most dendrograms. As *Bisifusarium* and FFSC (EPM4098, EPM4131, EPM4350, and EPM4351) were less represented in the dataset, they may have suffered the effect of incongruence (Pompanon *et al.* 2005, Zhang & Hare 2012), although it was possible to calculate a satisfactory diversity index for these species.

Dimensionality reduction analyses by PCA were performed to allow 3D graphic visualization of the relationship among fusarioid samples (Fig. 6). The sum of the three principal components ranged from 30.0–34.1 %, reflecting the variability expected for fusaria. Combinations #1, #6, and #8 revealed the highest cumulative percentage (33.5 %, 34.1 %, and 33.8 %, respectively), and *Neocosmospora*, as well as *Fusarium* and *Bisifusarium*, were plotted in the 3D graphic. The standard profile of the plot was observed in most AFLP profiles, only combinations #4 and #7 were observed in mixed groups (Fig. 6). Additionally, combinations #1 and #6 could resolve species of *Bisifusarium* and *Fusarium* better than others (Fig. 6A, F).

Better AFLP-derived MST generated in BioNumerics v. 7.6 showed unrooted long trees (Total network length ranged from 1 728.30 – 2 499.41), demonstrating the high diversity revealed by AFLP markers tested here. Additionally, networks still defined the *Neocosmospora*-group for the majority of combinations, but some isolate-related diversity should be contributed to other groups, as observed in the AFLP-derived MST (Fig. 7). Because MST does not admit hypothetical entries in the analysis, like parsimony methods, better performance should be viewed when those AFLP markers are used in a large AFLP dataset, mainly including more samples from *Fusarium* and *Bisifusarium* (Posada & Crandall 2001, Vauterin & Vauterin 2006).

© 2025 Westerdijk Fungal Biodiversity Institute

Finally, all AFLP markers tested here allowed the evaluation of genetic diversity in all species studied, although some AFLP markers performed better than others. As expected, some markers fit better to some genera than others, but it is clear that combination #2 (EcoRI-AT/MseI-TA) and #5 (EcoRI-AT/MseI-AG) were applicable for all fusarioid species tested here. Alternatively, combinations #1 (EcoRI-GA/MseI-AG) and #6 (EcoRI-GA/MseI-TT) are helpful in specific studies that involve exclusively *Bisifusarium* and *Fusarium*, respectively, due to good performance in the diversity indices and unique analysis.

DISCUSSION

We developed a novel AFLP fingerprinting protocol through *in silico* analysis and then validated it *in vitro* using clinically relevant fusarioid fungi. These pathogens exhibit efficient adaptation to various environments, indicating exposure to selective pressures (Zhang *et al.* 2006, Short *et al.* 2011, Al-Maqtoofi & Thornton 2016, Graça *et al.* 2016).

To guide the development of the AFLP marker system for a more comprehensive understanding of evolutionary processes in fusarioid fungi, we accessed twenty genomes from the NCBI Genome database. We then conducted *in silico* prediction, identifying informative clusters within the marker systems, from which we selected eight combinations for *in vitro* fingerprinting. This *in silico* analysis approach has also proven valuable in developing marker systems for other medical fungi, such as *Sporothrix* and *Paracoccidioides* (de Carvalho *et al.* 2020, Roberto *et al.* 2021). Furthermore, studies have highlighted these tools' high accuracy and cost-effectiveness, reducing errors compared to solely relying on *in vitro* experimental approaches (Caballero & Quesada 2010, De Vos *et al.* 2014).

As anticipated, the genomic diversity of fusarioid fungi is extensive, with AFLP fingerprinting successfully elucidating genetic variations even within a dataset comprising 40 strains. Some primer combinations, notably #2, #3, and #5, exhibited superior efficacy in revealing genetic diversity within *Neocosmospora*, while others, particularly #2 and #6, were well-suited for investigating *Fusarium* species and *Bisifusarium* (#1 and #6).

Phylogenetic inference based on partial genes *tef1α* and *rpb2* proved effective in identifying species and providing some insights into the dataset's diversity. However, it is worth noting that MLST, which includes three or more genes, offers a more informative typing system than the two-gene system (Zhang *et al.* 2006, Al-Hatmi *et al.* 2016a). Of relevance, AFLP demonstrated performance comparable to that of these genetic markers and, in some cases, outperformed MLST (Debourgogne *et al.* 2012, Thomas *et al.* 2019). When we reconstructed the dendrograms from AFLP data, clusters directly aligned with the phylogenetic tree and were supported by excellent congruence index values. Approximately 30 % of the genetic information was concentrated within three principal components for the most informative AFLP systems. This compared well with the 40–70 % range that was observed in other fungi, such as *Fonsecaea*, *Histoplasma*, *Sporothrix*, and *Paracoccidioides* (Rodrigues *et al.* 2020, de Carvalho *et al.* 2021, Roberto *et al.* 2021, Guevara *et al.* 2022).

Studies involving AFLP of clinical samples of fusarioid fungi did not detect variability in these genetic groups, whether they derived from outbreaks or from unconnected infections. Al-Hatmi *et al.* (2016a) used AFLP and sequencing to detect variability in fusarioid fungi, although they found that species from the same "species complexes" such as *F. solani* SC (*Neocosmospora*), contained no significant variation. These observations lead us to consider that these fungi have a largely clonal mode of reproduction and low genetic variability in the assayed outbreaks (Al-Hatmi *et al.* 2016a, Carlesse *et al.* 2017). Our simulation, on the other hand, demonstrates that the random choice of selective bases can negatively impact the diversity estimated in epidemiological surveillance studies (de Carvalho *et al.* 2020, Roberto *et al.* 2021).

Levels of polymorphism can be quantitatively evaluated through the polymorphism information content (*PIC*) for dominant markers. Loci exhibiting variability with a *PIC* value close to 1 are considered highly favourable. Thus, *PIC* serves as an essential metric for gauging the informativeness of the marker system, and the moderately ranged *PIC* values observed (0.3474–0.3725), along with other related indices such as *D*, *E*, *H*, H_{avp}, *MI*, and *Rp*, lend substantial support to the utility of the panels developed here. In contrast, studies involving *F. oxysporum* and AFLP yielded lower *PIC* values, possibly stemming from limited variability within the utilized dataset or specific characteristics of the employed AFLP scheme (Silva *et al.* 2013).

While AFLP panels offer high sensitivity for detecting genetic polymorphisms, it is essential to acknowledge their inherent limitations (Marwal & Gaur 2020). AFLP relies on the selective amplification of DNA fragments using restriction enzymes and primers, which can introduce biases (Vos *et al.* 1995). These biases may include incomplete DNA digestion or preferential amplification of certain fragments. Additionally, AFLP markers are dominant, meaning they cannot differentiate between heterozygous and homozygous genotypes (Garcia *et al.* 2004). Although we employed a robust bioinformatics framework to minimize these issues through careful primer design and optimization (de Carvalho *et al.* 2020, Roberto *et al.* 2021), these inherent biases can still affect the interpretation of genetic diversity and phylogenetic relationships.

Importantly, our system exhibited performance comparable to that of a *Fusarium* simple sequence repeats (SSR)-based system, as evidenced in *PIC* values (Saleh *et al.* 2021). However, a key distinction lies in the fact that AFLP systems offer more significant and effective multiplex ratios. This is attributed to the fact that the multiplex information in AFLP relies on combinations of various loci (fragments), whereas SSR may be confined to a few loci (Prevost & Wilkinson 1999, Varshney *et al.* 2007).

Although the most clinically relevant species were *Neocosmospora* spp., other species, such as those within *Bisifusarium* and *Fusarium s. str.*, have an epidemiology that is as yet not well understood. Combinations tested here revealed that #6 and #1 could describe variability in that dataset. The *F. oxysporum* SC was studied by several genotype methods, including AFLP (Baayen *et al.* 2000). The FOSC genotypes based on *tef1α*-IGS occasionally demonstrate a spread of clonal genotype ST33 related to human infections in nosocomial and community cases. Specimens bearing that sequence type have been described by Lombard *et al.* as the newly recognized species *F. veterinarium* (Lombard *et al.* 2019). Two samples included here (EPM4061 and EPM4133) were representative of *F. veterinarium*, and they present distinct genotypes in all markers system tested.

© 2025 Westerdijk Fungal Biodiversity Institute

Bisifusarium shows a complex epidemiological profile, perhaps due to its occurrence within domestic environments and its colonization of hydraulic structures within hospital settings (Schroers *et al.* 2009, Sautour *et al.* 2012, Al-Maqtoofi & Thornton 2016, Milanez *et al.* 2024). Considering this, the genetic diversity of *Bisifusarium* remains largely uncharted, warranting dedicated studies or tools for investigation. In this context, we present a novel methodology to unravel the population dynamics inherent to *Bisifusarium* spp.

The robust reproducibility we observed in our fingerprinting experiments, combined with improved precision, significantly boosts the reliability and accuracy of genotyping systems available to study fusarioid fungal pathogens, including those that infect humans. Developing new AFLP systems also extends its potential applications to various epidemiological investigations involving these agents. One key factor contributing to the cost-effectiveness of AFLP is its selective PCR amplification process that utilizes a limited number of primers. This results in lower reagent costs than techniques requiring a more extensive set of primers or probes. For a more detailed examination of *Neocosmospora*'s finer-scale epidemiological patterns, we recommend the use of combination #2. Conversely, for a meticulous analysis of other medically relevant fusarioid fungi, we suggest considering combinations #1 or #6. The novel genetic panels we describe can be used wisely as a high-throughput technology, expediting the assessment of intraspecific variability across fusarioid species amid ongoing disease outbreaks.

ACKNOWLEDGEMENTS

The authors acknowledge the financial support granted by the São Paulo Research Foundation (FAPESP 2017/27265-5 and FAPESP 2018/21460-3), National Council for Scientific and Technological Development (CNPq 433276/2018-5), The National Institute of Science and Technology in Human Pathogenic Fungi, Brazil (CNPq 405934/2022-0), and Coordination for the Improvement of Higher Education Personnel (CAPES 88887.159096/2017-00). AMR is a CNPq Research Productivity Fellow (CNPq 314089/2023-3). MCF was funded by the UK Medical Research Council and Wellcome Trust and is a Fellow in the CIFAR 'Fungal Kingdoms' program. The funders had no role in the study design, data collection, analysis, decision to publish, or manuscript preparation.

Institutional review board statement: The study was conducted according to the guidelines of the Declaration of Helsinki and approved by the Ethics Committee of the Federal University of São Paulo (protocol 3147220120; 17 February 2020).

Conflict of interest: The authors declare that there is no conflict of interest.

REFERENCES

Al-Hatmi AM, Hagen F, Menken SB, *et al.* (2016a). Global molecular epidemiology and genetic diversity of *Fusarium*, a significant emerging group of human opportunists from 1958 to 2015. *Emerging Microbes & Infections* **5**: e124–e124.

Al-Hatmi AM, Mirabolfathy M, Hagen F, *et al.* (2016b). DNA barcoding, MALDI-TOF, and AFLP data support *Fusarium ficicrescens* as a distinct species within the *Fusarium fujikuroi* species complex. *Fungal Biology* **120**: 265–278.

Al-Maqtoofi M, Thornton CR (2016). Detection of human pathogenic *Fusarium* species in hospital and communal sink biofilms by using a highly specific monoclonal antibody. *Environmental Microbiology* **18**: 3620–3634.

Al-Reedy RM, Malireddy R, Dillman CB, *et al.* (2012). Comparative analysis of *Fusarium* mitochondrial genomes reveals a highly variable region that encodes an exceptionally large open reading frame. *Fungal Genetics and Biology* **49**: 2–14.

Amiryousefi A, Hyvonen J, Poczai P (2018). iMEC: online marker efficiency calculator. *Applications in Plant Sciences* **6**: e01159.

Baayen RP, O'Donnell K, Bonants PJ, *et al.* (2000). Gene genealogies and AFLP analyses in the *Fusarium oxysporum* complex identify monophyletic and nonmonophyletic *formae speciales* causing wilt and rot disease. *Phytopathology* **90**: 891–900.

Babicki S, Arndt D, Marcu A, *et al.* (2016). Heatmapper: web-enabled heat mapping for all. *Nucleic Acids Research* **44**: W147–153.

Bain JM, Tavanti A, Davidson AD, *et al.* (2007). Multilocus sequence typing of the pathogenic fungus *Aspergillus fumigatus*. *Journal of Clinical Microbiology* **45**: 1469–1477.

Bandelt HJ, Forster P, Röhl A (1999). Median-joining networks for inferring intraspecific phylogenies. *Molecular Biology and Evolution* **16**: 37–48.

Barros G, Zanon MS, Abod A, *et al.* (2012). Natural deoxynivalenol occurrence and genotype and chemotype determination of a field population of the *Fusarium graminearum* complex associated with soybean in Argentina. *Food Additives & Contaminants. Part A Chemistry, Analysis, Control, Exposure & Risk Assessment* **29**: 293–303.

Bhunjun CS, Chen YJ, Phukhamsakda C, *et al.* (2024). What are the 100 most cited fungal genera? *Studies in Mycology* **108**: 1–411.

Bonin A, Bellemain E, Bronken Eidesen P, *et al.* (2004). How to track and assess genotyping errors in population genetics studies. *Molecular Ecology* **13**: 3261–3273.

Botstein D, White RL, Skolnick M, *et al.* (1980). Construction of a genetic linkage map in man using restriction fragment length polymorphisms. *The American Journal of Human Genetics* **32**: 314–331.

Caballero A, Quesada H (2010). Homoplasy and distribution of AFLP fragments: An analysis *in silico* of the genome of different species. *Molecular Biology and Evolution* **27**: 1139–1151.

Carlesse F, Amaral AC, Gonçalves SS, *et al.* (2017). Outbreak of *Fusarium oxysporum* infections in children with cancer: An experience with 7 episodes of catheter-related fungemia. *Antimicrobial Resistance & Infection Control* **6**: 93.

Casanova A, Maroso F, Blanco A, *et al.* (2021). Low impact of different SNP panels from two building-loci pipelines on RAD-Seq population genomic metrics: case study on five diverse aquatic species. *BMC Genomics* **22**: 150.

Chen Y, Frazzitta AE, Litvintseva AP, *et al.* (2015). Next generation multilocus sequence typing (NGMLST) and the analytical software program MLSTEZ enable efficient, cost-effective, high-throughput, multilocus sequencing typing. *Fungal Genetics and Biology* **75**: 64–71.

Coleman JJ, Rounsley SD, Rodriguez-Carres M, *et al.* (2009). The genome of *Nectria haematococca*: Contribution of supernumerary chromosomes to gene expansion. *PLoS Genetics* **5**: e1000618.

© 2025 Westerdijk Fungal Biodiversity Institute

Cuomo CA, Güldener U, Xu JR, *et al.* (2007). The *Fusarium graminearum* genome reveals a link between localized polymorphism and pathogen specialization. *Science* **317**: 1400–1402.

de Carvalho JA, Beale MA, Hagen F, *et al.* (2021). Trends in the molecular epidemiology and population genetics of emerging *Sporothrix* species. *Studies in Mycology* **100**: 100129.

de Carvalho JA, Hagen F, Fisher MC, *et al.* (2020). Genome-wide mapping using new AFLP markers to explore intraspecific variation among pathogenic *Sporothrix* species. *PLoS Neglected Tropical Diseases* **14**: e0008330.

de Oliveira Rocha L, Reis GM, da Silva VN, *et al.* (2011). Molecular characterization and fumonisin production by *Fusarium verticillioides* isolated from corn grains of different geographic origins in Brazil. *International Journal of Food Microbiology* **145**: 9–21.

de Vienne DM, Giraud T, Martin OC (2007). A congruence index for testing topological similarity between trees. *Bioinformatics* **23**: 3119–3124.

De Vos L, Steenkamp ET, Martin SH, *et al.* (2014). Genome-wide macrosynteny among *Fusarium* species in the *Gibberella fujikuroi* complex revealed by Amplified Fragment Length Polymorphisms. *PLoS ONE* **9**: e114682.

Dean R, Van Kan JA, Pretorius ZA, *et al.* (2012). The top 10 fungal pathogens in molecular plant pathology. *Molecular Plant Pathology* **13**: 414–430.

Debourgogne A, Gueidan C, de Hoog S, *et al.* (2012). Comparison of two DNA sequence-based typing schemes for the *Fusarium solani* species complex and proposal of a new consensus method. *Journal of Microbiological Methods* **91**: 65–72.

Debourgogne A, Gueidan C, Hennequin C, *et al.* (2010). Development of a new MLST scheme for differentiation of *Fusarium solani* species complex (FSSC) isolates. *Journal of Microbiological Methods* **82**: 319–323.

Diniz-Filho JA, Soares TN, Lima JS, *et al.* (2013). Mantel test in population genetics. *Genetics and Molecular Biology* **36**: 475–485.

Edel-Hermann V, Sautour M, Gautheron N, *et al.* (2016). A clonal lineage of *Fusarium oxysporum* circulates in the tap water of different French hospitals. *Applied Environmental Microbiology* **82**: 6483–6489.

Garcia AA, Benchimol LL, Barbosa AM, *et al.* (2004). Comparison of RAPD, RFLP, AFLP and SSR markers for diversity studies in tropical maize inbred lines. *Genetics and Molecular Biology* **27**: 579–588.

Godoy P, Cano J, Gené J, *et al.* (2004). Genotyping of 44 isolates of *Fusarium solani*, the main agent of fungal keratitis in Brazil. *Journal of Clinical Microbiology* **42**: 4494–4497.

Graça MG, van der Heijden IM, Perdigão L, *et al.* (2016). Evaluation of two methods for direct detection of *Fusarium* spp. in water. *Journal of Microbiological Methods* **123**: 39–43.

Guevara A, Nery AF, de Souza Carvalho Melhem M, *et al.* (2022). Molecular epidemiology and clinical-laboratory aspects of chromoblastomycosis in Mato Grosso, Brazil. *Mycoses* **65**: 1146–1158.

Herr JR, Scully ED, Geib SM, *et al.* (2016). Genome sequence of *Fusarium* isolate MYA-4552 from the midgut of *Anoplophora glabripennis*, an invasive, wood-boring beetle. *Genome Announcements* **4**: e00544-16.

Hillis DM, Bull JJ (1993). An empirical test of bootstrapping as a method for assessing confidence in phylogenetic analysis. *Systematic Biology* **42**: 182–192.

Huang X, Das A, Sahu BB, *et al.* (2016). Identification of highly variable supernumerary chromosome segments in an asexual pathogen. *PLoS ONE* **11**: e0158183.

Jureen R, Koh TH, Wang G, *et al.* (2008). Use of multiple methods for genotyping *Fusarium* during an outbreak of contact lens associated fungal keratitis in Singapore. *BMC Infectious Diseases* **8**: 92.

Kerényi Z, Moretti A, Waalwijk C, *et al.* (2004). Mating type sequences in asexually reproducing *Fusarium* species. *Applied Environmental Microbiology* **70**: 4419–4423.

Kimura M (1980). A simple method for estimating evolutionary rates of base substitutions through comparative studies of nucleotide sequences. *Journal of Molecular Evolution* **16**: 111–120.

Kumar S, Stecher G, Tamura K (2016). MEGA7: Molecular Evolutionary Genetics Analysis Version 7.0 for Bigger Datasets. *Molecular Biology and Evolution* **33**: 1870–1874.

Laraba I, McCormick SP, Vaughan MM, *et al.* (2021). Phylogenetic diversity, trichothecene potential, and pathogenicity within *Fusarium sambucinum* species complex. *PLoS ONE* **16**: e0245037.

Lee J, Chang IY, Kim H, *et al.* (2009). Genetic diversity and fitness of *Fusarium graminearum* populations from rice in Korea. *Applied Environmental Microbiology* **75**: 3289–3295.

Leslie JF, Summerell BA (2006). *The Fusarium laboratory manual*. Blackwell Pub., Ames, Iowa: 416.

Li Y, Steenwyk JL, Chang Y, *et al.* (2021). A genome-scale phylogeny of the kingdom *Fungi*. *Current Biology* **31**: 1653–1665.

Liu BH (1998). *Statistical genomics: linkage, mapping, and QTL analysis*. CRC press, Boca Raton.

Liu X, Xing M, Kong C, *et al.* (2019). Genetic diversity, virulence, race profiling, and comparative genomic analysis of the *Fusarium oxysporum f. sp. conglutinans* strains infecting cabbages in China. *Frontiers in Microbiology* **10**: 1373.

Lombard L, Sandoval-Denis M, Lamprecht SC, *et al.* (2019). Epitypification of *Fusarium oxysporum* — clearing the taxonomic chaos. *Persoonia* **43**: 1–47.

Lysøe E, Frandsen RJN, Divon HH, *et al.* (2016). Draft genome sequence and chemical profiling of *Fusarium langsethiae*, an emerging producer of type A trichothecenes. *International Journal of Food Microbiology* **221**: 29–36.

Lysøe E, Harris LJ, Walkowiak S, *et al.* (2014). The genome of the generalist plant pathogen *Fusarium avenaceum* is enriched with genes involved in redox, signaling and secondary metabolism. *PLoS ONE* **9**: e112703.

Mantel N (1967). The detection of disease clustering and a generalized regression approach. *Cancer Research* **27**: 209–220.

Marwal A, Gaur RK (2020). Molecular markers: tool for genetic analysis. In: *Animal Biotechnology* (Second Edition), (Verma AS, Singh A, eds), Academic Press, Boston: 353–372.

Milanez EPR, de Souza P, Monteiro RC, *et al.* (2024). Fusarium keratitis in a Brazilian tropical semi-arid area: Clinical-epidemiological features, molecular identification and antifungal susceptibility. *Mycoses* **67**: e13728.

Moretti ML, Busso-Lopes AF, Tararam CA, *et al.* (2018). Airborne transmission of invasive fusariosis in patients with hematologic malignancies. *PLoS ONE* **13**: e0196426.

Mueller UG, Wolfenbarger LL (1999). AFLP genotyping and fingerprinting. *Trends in Ecology & Evolution* **14**: 389–394.

Nei M (1987). *Molecular evolutionary genetics*. Columbia University Press, New York: 512.

Niehaus EM, Kim HK, Münsterkötter M, *et al.* (2017). Comparative genomics of geographically distant *Fusarium fujikuroi* isolates revealed two distinct pathotypes correlating with secondary metabolite profiles. *PLoS Pathogens* **13**: e1006670.

Nucci M, Varon AG, Garnica M, *et al.* (2013). Increased incidence of invasive fusariosis with cutaneous portal of entry, Brazil. *Emerging Infectious Diseases* **19**: 1567–1572.

© 2025 Westerdijk Fungal Biodiversity Institute

O'Donnell K, Gueidan C, Sink S, *et al.* (2009). A two-locus DNA sequence database for typing plant and human pathogens within the *Fusarium oxysporum* species complex. *Fungal Genetics and Biology* **46**: 936–948.

O'Donnell K, Kistler HC, Cigelnik E, *et al.* (1998). Multiple evolutionary origins of the fungus causing Panama disease of banana: Concordant evidence from nuclear and mitochondrial gene genealogies. *Proceedings of the National Academy of Sciences USA* **95**: 2044–2049.

O'Donnell K, Sarver BA, Brandt M, *et al.* (2007). Phylogenetic diversity and microsphere array-based genotyping of human pathogenic Fusaria, including isolates from the multistate contact lens-associated U.S. keratitis outbreaks of 2005 and 2006. *Journal of Clinical Microbiology* **45**: 2235–2248.

O'Donnell K, Sutton DA, Rinaldi MG, *et al.* (2004). Genetic diversity of human pathogenic members of the *Fusarium oxysporum* complex inferred from multilocus DNA sequence data and amplified fragment length polymorphism analyses: evidence for the recent dispersion of a geographically widespread clonal lineage and nosocomial origin. *Journal of Clinical Microbiology* **42**: 5109–5120.

O'Donnell K, Sutton DA, Wiederhold N, *et al.* (2016). Veterinary fusarioses within the United States. *Journal of Clinical Microbiology* **54**: 2813–2819.

Oksanen J, Blanchet FG, Friendly M, *et al.* (2019). *Package 'vegan'*. Community ecology package, version 2.5–7.

Pompanon F, Bonin A, Bellemain E, *et al.* (2005). Genotyping errors: causes, consequences and solutions. *Nature Reviews Genetics* **6**: 847–859.

Ponts N, Gautier C, Gouzy J, *et al.* (2020). Evolution of *Fusarium tricinctum* and *Fusarium avenaceum* mitochondrial genomes is driven by mobility of introns and of a new type of palindromic microsatellite repeats. *BMC Genomics* **21**: 358.

Posada D, Crandall KA (2001). Intraspecific gene genealogies: Trees grafting into networks. *Trends in Ecological Evolution* **16**: 37–45.

Powell W, Morgante M, Andre C, *et al.* (1996). The comparison of RFLP, RAPD, AFLP and SSR (microsatellite) markers for germplasm analysis. *Molecular Breeding* **2**: 225–238.

Prevost A, Wilkinson MJ (1999). A new system of comparing PCR primers applied to ISSR fingerprinting of potato cultivars. *Theoretical and Applied Genetics* **98**: 107–112.

Qin M, Zhang N, Zhu S*, et al.* (2021). Development of polymorphic microsatellite markers for the tertiary relict tree species *Taiwania cryptomerioides* (*Cupressaceae*) in East Asia. *Molecular Biology Reports* **48**: 3031–3036.

Ramirez ML, Reynoso MM, Farnochi MC, *et al.* (2007). Population genetic structure of *Gibberella zeae* isolated from wheat in Argentina. *Food Additives & Contaminants* **24**: 1115–1120.

Roberto TN, De Carvalho JA, Beale MA, *et al.* (2021). Exploring genetic diversity, population structure, and phylogeography in *Paracoccidioides* species using AFLP markers. *Studies in Mycology* **100**: 100131.

Rodrigues AM, Beale MA, Hagen F, *et al.* (2020). The global epidemiology of emerging *Histoplasma* species in recent years. *Studies in Mycology* **97**: 100095.

Rombauts S, Van De Peer Y, Rouze P (2003). AFLPinSilico, simulating AFLP fingerprints. *Bioinformatics* **19**: 776–777.

Rozas J, Ferrer-Mata A, Sánchez-DelBarrio JC, *et al.* (2017). DnaSP 6: DNA sequence polymorphism analysis of large data sets. *Molecular Biology and Evolution* **34**: 3299–3302.

Salah H, Al-Hatmi AM, Theelen B, *et al.* (2015). Phylogenetic diversity of human pathogenic *Fusarium* and emergence of uncommon virulent species. *Journal of Infection* **71**: 658–666.

Saleh AA, Sharafaddin AH, El Komy MH, *et al.* (2021). Molecular and physiological characterization of *Fusarium* strains associated with different diseases in date palm. *PLoS ONE* **16**: e0254170.

Sautour M, Edel-Hermann V, Steinberg C, *et al.* (2012). *Fusarium* species recovered from the water distribution system of a French university hospital. *International Journal of Hygiene and Environmental Health* **215**: 286–292.

Sayers EW, Bolton EE, Brister JR, *et al.* (2022). Database resources of the national center for biotechnology information. *Nucleic Acids Research* **50**: D20–D26.

Schroers HJ, O'Donnell K, Lamprecht SC, *et al.* (2009). Taxonomy and phylogeny of the *Fusarium dimerum* species group. *Mycologia* **101**: 44–70.

Sharma R, Thakur RP, Senthilvel S, *et al.* (2011). Identification and characterization of toxigenic fusaria associated with sorghum grain mold complex in India. *Mycopathologia* **171**: 223–230.

Shiraishi A, Leslie JF, Zhong S, *et al.* (2012). AFLP, pathogenicity, and VCG analyses of *Fusarium oxysporum* and *Fusarium pseudocircinatum* from *Acacia koa*. *Plant Disease* **96**: 1111–1117.

Short DP, O'Donnell K, Zhang N, *et al.* (2011). Widespread occurrence of diverse human pathogenic types of the fungus *Fusarium* detected in plumbing drains. *Journal of Clinical Microbiology* **49**: 4264–4272.

Silva AdS, Oliveira EJd, Haddad F, *et al.* (2013). Molecular fingerprinting of *Fusarium oxysporum f. sp. passiflorae* isolates using AFLP markers. *Scientia Agricola* **70**: 108–115.

Suga H, Gale L, Kistler H (2004). Development of VNTR markers for two *Fusarium graminearum* clade species. *Molecular Ecology Notes* **4**: 468–470.

Tessier C, David J, This P, *et al.* (1999). Optimization of the choice of molecular markers for varietal identification in *Vitis vinifera* L. *Theoretical and Applied Genetics* **98**: 171–177.

Thomas B, Contet Audonneau N, Machouart M, *et al.* (2019). Molecular identification of *Fusarium* species complexes: Which gene and which database to choose in clinical practice? *Journal de Mycologie Médicale* **29**: 56–58.

van Dam P, de Sain M, Ter Horst A, *et al.* (2018). Use of comparative genomics-based markers for discrimination of host specificity in *Fusarium oxysporum*. *Applied Environmental Microbiology* **84**: e01868–01817.

van Dam P, Rep M (2017). The distribution of miniature impala elements and six genes in the *Fusarium* genus is suggestive of horizontal gene transfer. *Journal of Molecular Evolution* **85**: 14–25.

van Diepeningen AD, Feng P, Ahmed S, *et al.* (2015). Spectrum of *Fusarium* infections in tropical dermatology evidenced by multilocus sequencing typing diagnostics. *Mycoses* **58**: 48–57.

Varshney RK, Chabane K, Hendre PS, *et al.* (2007). Comparative assessment of EST-SSR, EST-SNP and AFLP markers for evaluation of genetic diversity and conservation of genetic resources using wild, cultivated and elite barleys. *Plant Science* **173**: 638–649.

Vauterin L, Vauterin P (2006). Integrated databasing and analysis. In: *Molecular Identification, Systematics, and Population Structure of Prokaryotes* (Stackebrandt E, ed), Springer Berlin Heidelberg, Berlin, Heidelberg: 141–217.

Vos P, Hogers R, Bleeker M, *et al.* (1995). AFLP: a new technique for DNA fingerprinting. *Nucleic Acids Research* **23**: 4407–4414.

Wu F (2007). Measuring the economic impacts of *Fusarium* toxins in animal feeds. *Animal Feed Science and Technology* **137**: 363–374.

Xie SY, Ma T, Zhao N, *et al.* (2022). Whole-genome sequencing and comparative genome analysis of *Fusarium solani-melongenae* causing Fusarium root and stem rot in sweetpotatoes. *Microbiology Spectrum* **10**: e0068322.

© 2025 Westerdijk Fungal Biodiversity Institute

Zeller KA, Bowden RL, Leslie JF (2003). Diversity of epidemic populations of *Gibberella zeae* from small quadrats in Kansas and North Dakota. *Phytopathology* **93**: 874–880.

Zhang H, Hare MP (2012). Identifying and reducing AFLP genotyping error: an example of tradeoffs when comparing population structure in broadcast spawning versus brooding oysters. *Heredity* **108**: 616–625.

Zhang N, O'Donnell K, Sutton DA, *et al.* (2006). Members of the *Fusarium solani* species complex that cause infections in both humans and plants are common in the environment. *Journal of Clinical Microbiology* **44**: 2186–2190.

Supplementary Material: http://fuse-journal.org/

Fig. S1. Similarity values correlation computed with the Mantel Test. The diagonal has plotted similarity matrices. Squares on the upper side of the diagonal show correlation values (r). Those on the lower side show corresponding correlation plots.

Fig. S2. Experimental congruence between AFLP markers. The diagonal has plotted similarity matrices. Squares above the diagonal show correlation values (r). The squares below show correlation plots. The correlation cladogram is at right.

Table S1. Diversity indices computed from AFLP fingerprinting.

Table S2. Comparison results from Mantel test.

Table S3. Pearson correlation for experimental congruence.

Table S4. Diversity indices for each species included in the study.

© 2025 Westerdijk Fungal Biodiversity Institute